Cell Reports

Report

Insights into convergent evolution of cosexuality in liverworts from the *Marchantia quadrata* genome

Graphical abstract

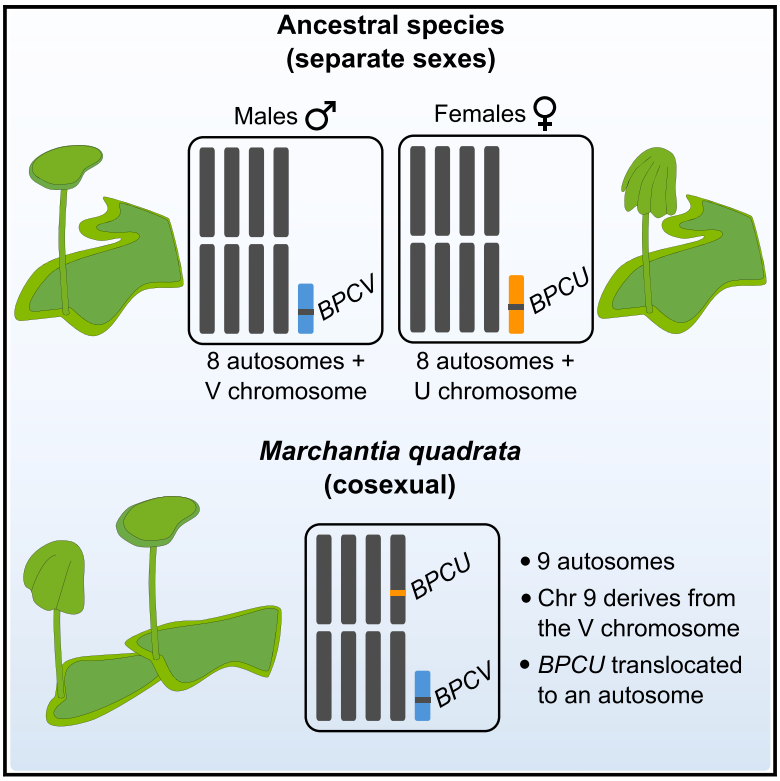

Highlights

- Liverworts evolving cosexuality retain the male (V) but lose the female (U) sex chromosome
- Essential genes of the U chromosome are maintained on the autosomes
- The feminizer gene acquires new regulation to enable both male and female functions
- Evolution of cosexuality followed a similar pattern twice independently in liverworts

Authors

Giacomo Potente, Yukiko Yasui, Eita Shimokawa, ..., Masaki Shimamura, Takayuki Kohchi, Péter Szövényi

Correspondence

yasui.yukiko.7a@kyoto-u.ac.jp (Y.Y.), peter.szoevenyi@uzh.ch (P.S.)

In brief

Potente et al. show that in the liverwort *M. quadrata*, the evolution of cosexuality involves the retention of the male (V) sex chromosome and the complete loss of the female (U) sex chromosome. This pattern parallels observations in another species, suggesting that transitions to cosexuality may be predictable in liverworts.

Potente et al., 2025, Cell Reports *44*, 115503
April 22, 2025
https://doi.org/10.1016/j.celrep.2025.115503

CellPress

Cell Reports

CellPress
OPEN ACCESS

Report

Insights into convergent evolution of cosexuality in liverworts from the *Marchantia quadrata* genome

Giacomo Potente,[1,2,10] Yukiko Yasui,[3,10,*] Eita Shimokawa,[3] Jerry Jenkins,[4] Rachel N. Walstead,[4] Jane Grimwood,[4] Jeremy Schmutz,[4,6] Jim Leebens-Mack,[5] Tomas Bruna,[6] Navneet Kaur,[6] Raymond Lee,[6] Sumaira Zama,[6] Tomoha Tanaka,[3] Yuka Umeya,[3] Shogo Kawamura,[3] Katsuyuki T. Yamato,[7] Katsushi Yamaguchi,[8] Shuji Shigenobu,[8] Masaki Shimamura,[9] Takayuki Kohchi,[3] and Péter Szövényi[1,2,11,*]

[1]Department of Systematic and Evolutionary Botany, University of Zurich, Zollikerstr. 107, 8008 Zurich, Switzerland
[2]Zurich-Basel Plant Science Center, ETH Zurich, Tannenstrasse 1, 8092 Zürich, Switzerland
[3]Graduate School of Biostudies, Kyoto University, Sakyo-ku, Kyoto 606-8502, Japan
[4]HudsonAlpha Institute for Biotechnology, 601 Genome Way, Huntsville, AL, USA
[5]Department of Plant Biology and The Plant Center, University of Georgia, 120 Carlton Street, Suite 2502, Athens, GA 30602, USA
[6]Lawrence Berkeley National Laboratory, Department of Energy Joint Genome Institute, Berkeley, CA 94720, USA
[7]Faculty of Biology-Oriented Science and Technology (BOST), Kindai University, Kinokawa, Wakayama 649-6493, Japan
[8]Trans-Omics Faculty, National Institute for Basic Biology, Okazaki, Aichi 444-8585, Japan
[9]Graduate School of Integrated Science for Life, Hiroshima University, Higashi-Hiroshima, Hiroshima 739-8526, Japan
[10]These authors contributed equally
[11]Lead contact
*Correspondence: yasui.yukiko.7a@kyoto-u.ac.jp (Y.Y.), peter.szoevenyi@uzh.ch (P.S.)
https://doi.org/10.1016/j.celrep.2025.115503

SUMMARY

Sex chromosomes are expected to coevolve with their respective sex, potentially disfavoring their co-occurrence as cosexuality evolves. This effect is expected to be stronger where sex chromosomes are restricted to one sex, such as in plants expressing sex in their haploid stage. We assess this hypothesis in liverworts with U/V sex chromosomes, ancestral dioicy, and several independent transitions to monoicy (cosexuality). We report the chromosome-level genome assembly of *Marchantia quadrata*, which recently evolved monoicy, and perform comparative genomic analyses with its dioicous relative *M. polymorpha*. We find that monoicy evolved via retention of the V chromosome as a small ninth chromosome, complete loss of the U chromosome, and translocation of key U-linked genes to autosomes, among which the major sex-determining gene (*Feminizer*) acquired environmental/developmental regulation. Our findings parallel recent observations on *Ricciocarpos natans*, which evolved monoicy independently, suggesting genetic constraints that may make transitions to monoicy predictable in liverworts.

INTRODUCTION

In eukaryotes, sexual function may be partitioned between males and females (in species with separate sexes) or co-occur within each individual (in cosexual species). Evolutionary transitions between these reproductive systems are common, with the shift from cosexuality to separate sexes being well studied.[1–3] In contrast, the evolutionary trajectory from separate sexes to cosexual species remains less understood.[4–6]

Sex is often determined by sex chromosomes. These originate from a pair of autosomes starting to diverge by acquiring a non-recombining sex-determining region and are expected to accumulate genes/alleles beneficial to one but detrimental to the other sex.[7–10] This often leads to sex-specific gene regulatory networks,[11] posing a challenge to the evolution of cosexuality from separate sex ancestors.[12,13] This is because, in cosexual organisms descended from unisexual ancestors, male and female sexual functions enabled by the sex chromosomes must be present in each individual, while sexually antagonistic effects of the sex chromosomes should also be minimized. Consequently, theory predicts that the co-occurrence of both sex chromosomes should be disfavored by natural selection in the evolution of cosexuality.[14,15] The accumulation of sexually antagonistic alleles is expected to be especially pronounced on sex chromosomes restricted to one sex.[16–19] In a number of eukaryotic photosynthetic organisms, such as green algae, brown algae, and bryophytes, sex chromosomes are restricted to their respective sex because sex is expressed in the haploid life cycle stage and is determined by the presence of a single U (female) or V (male) chromosome.[17] Indeed, recent observations suggest that in some organisms with U/V sex chromosomes, components of a single sex chromosome may be preferentially retained as cosexuality evolves.[12,13,20,21] However, detailed information on multiple independent evolutionary transitions is scarce, making it difficult to draw general conclusions.

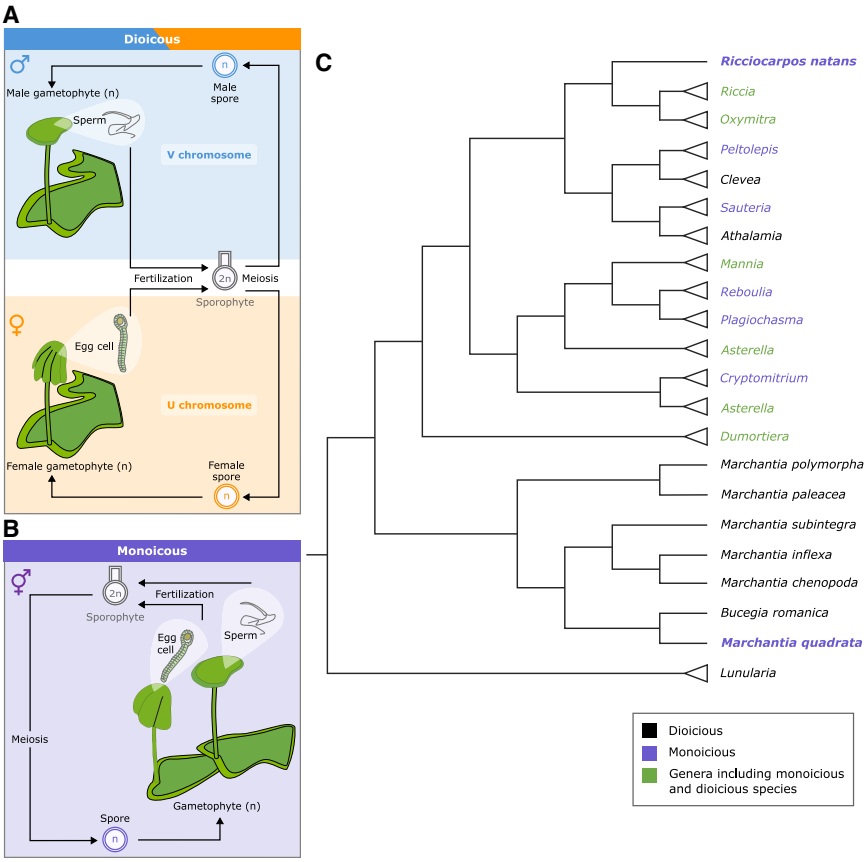

Figure 1. The life cycle of dioicous and monoicous liverworts and their phylogenetic distribution in the clade containing *M. quadrata* and *R. natans*

(A) In dioicous species, e.g., *M. polymorpha*, distinct male and female individuals possess sex chromosomes (V chromosome or U chromosome, respectively) and develop male or female reproductive receptacles, respectively, from the meristem region at the apex, which contains a stem cell. Fertilization occurring between a sperm produced by a (haploid) male gametophyte and an egg cell produced by a (haploid) female gametophyte results in a (diploid) sporophyte. Through meiosis, the sporophyte can produce either male or female spores, which will develop into male or female individuals.

(B) In monoicous species, e.g., *M. quadrata*, the same individual can produce male and female receptacles, i.e., sperms and egg cells. In *M. quadrata*, new thalli frequently emerge from the ventral side of older thalli, and male and female reproductive receptacles develop on separate thalli in such a way that older and younger thalli have alternating sexes. The sporophyte resulting from fertilization can produce only one type of spore, which will result in a cosexual individual.

(C) Phylogenetic relationship and sexual systems in the liverwort clade, including *R. natans* and *M. quadrata*. Strictly dioicous and monoicous taxa are shown in black and purple, respectively. Genera described as having both monoicous and dioicous species are colored in green. The only two monoicous species in which the transition to cosexuality was investigated, i.e., *M. quadrata* and *R. natans*, are shown in bold font. The phylogenetic tree was redrawn from Villarreal A et al.[29]

In liverworts, separate sexes (dioicy) are the ancestral condition, and sex is determined by haploid U and V chromosomes, whose structure, gene content, and the mechanism of sex determination are well understood.[22–26] The transition to cosexuality (monoicy) has occurred independently multiple times in liverworts,[27] and, in line with theory, a previous study in *Ricciocarpos natans* (Figure 1) reported that monoicy evolved via retention of the V and loss of the U chromosomes and the translocation of U-linked genes to autosomes.[21] To assess the repeatability of this pattern, we investigated genomic and regulatory changes associated with the evolution of cosexuality in another liverwort, *Marchantia quadrata,* which independently evolved monoicy about 10 mya[28,29] (Figure 1). Our comparative analysis implies that genomic changes associated with the dioicy-to-monoicy transition in these species are very similar and, thus, may be predictable. Furthermore, we show that in *M. quadrata*, the major sex-determining gene (*BPCU*/*Feminizer*) has acquired environmental and/or developmental regulation, enabling the alternate production of male and female reproductive structures within the same individual. This finding provides new insights into the fate of liverwort sex chromosomes and sex-determining genes during the transition to monoicy and, more broadly, on the genetic underpinnings of the evolution of cosexuality.

RESULTS AND DISCUSSION

Evolution of cosexuality involves the retention of the male (V) and the loss of the female (U) sex chromosomes

Using a combination of PacBio sequencing and Hi-C scaffolding, we assembled the *M. quadrata* genome into nine chromosomes, most of which contain telomeric sequences on both ends (Figure 2; Tables S1 and S2). We also assembled its chloroplast and mitochondrial genomes (Figure S1). Similar to the related dioicous *Marchantia polymorpha*,[30,31] the monoicous *M. quadrata* genome composed of eight large (84.4–116.1 Mb in length) chromosomes and a smaller (25.9 Mb) chromosome, referred to as chromosome 9[28] (Figure 2). The eight large chromosomes are syntenic to the autosomes of *M. polymorpha*, whereas chromosome 9 is not syntenic to any *M. polymorpha* chromosome but exhibits several characteristics typical of sex chromosomes: it is rich in repetitive sequences, gene poor, and displays a condensed chromatin three-dimensional structure (Figures 2, 3A, and 3C; Table S3). To determine whether chromosome 9 derived from the U or V sex chromosome (or a fusion of both) of the common ancestor shared by *M. polymorpha* and *M. quadrata*, we searched for homologs of the *M. quadrata* chromosome 9 genes in *M. polymorpha*. Of the 45 genes found on chromosome 9, 25 were homologs of either V-specific genes or genes with both U and V alleles (so-called

CellPress
OPEN ACCESS

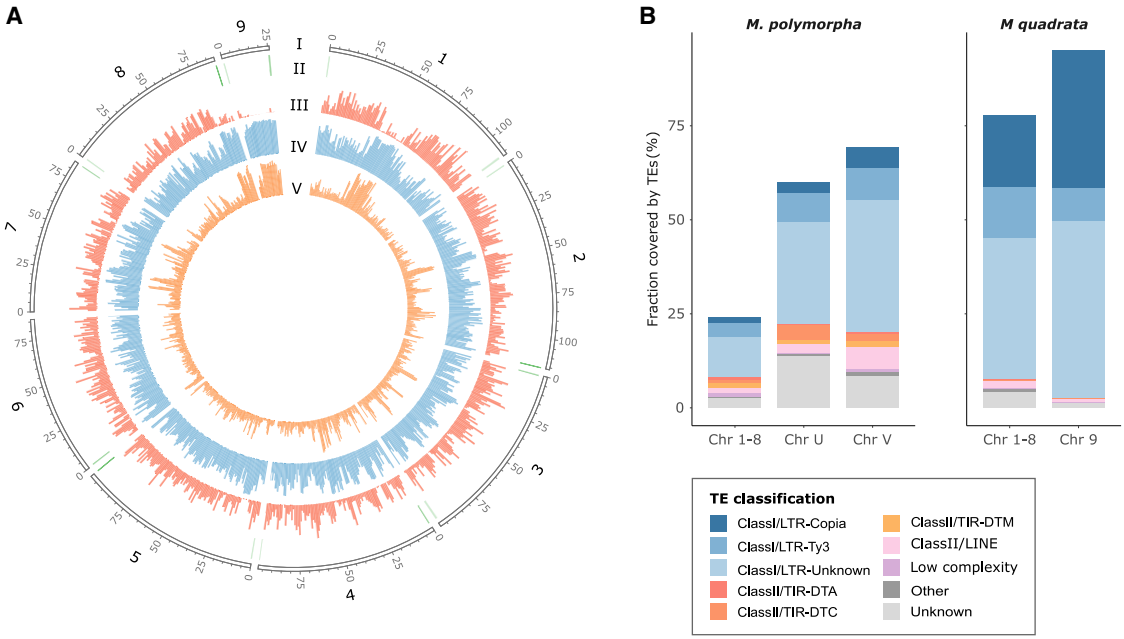

Figure 2. Summary of the *M. quadrata* genome and comparison with *M. polymorpha*

(A) Circos plot showing, from outside to inside, (I) the nine chromosomes of *M. quadrata*, with ticks every 5 Mb; (II) telomeric repeats (green); (III) gene density (red); (IV) transposable element (TE) density (blue); and (V) Copia LTR-RT density (orange). Tracks II–V were calculated in 1 Mb windows.

(B) TE content of the *M. polymorpha* and *M. quadrata* genomes. For both species, the fraction of sequence covered by each TE family is reported and colored as indicated in the legend.

gametologs), and none were homologous to U-specific genes of *M. polymorpha* (Table S4). Reconstructing phylogenies including *M. polymorpha* gametologs and their *M. quadrata* homologs revealed that 16 out of the 23 *M. quadrata* homologs of the *M. polymorpha* gametologs occurred on chromosome 9, and 13 of these represented the V-allele (Figure S2; Table S4). Furthermore, *M. quadrata* contained 14 orthologs of V-gametologs and 16 homologs of V-specific genes out of the 92 V-linked genes of *M. polymorpha* but only 3 orthologs of U-gametologs and one homolog of U-specific genes out of 63 U-linked genes. Collectively, these observations indicate that chromosome 9 of *M. quadrata* derived from the V chromosome, while the U chromosome was lost during the transition from dioicy to monoicy, after transferring four genes to autosomes (Figures 3B; Table S4). We note that three of these four U-genes are on *M. quadrata* chromosome 4, raising the possibility that they translocated in a single event.

Accessibility of male and female functions is enabled by the translocation of the *Feminizer* gene to the autosomes

In the dioicous *M. polymorpha*, sexual reproduction begins with the development of initial cells at thallus apices, which differentiate into either female or male gametangia, accompanied by the formation of reproductive receptacles in each of the female and male plants[32] (Figure S3). In contrast, in *M. quadrata*, each individual can produce both male and female reproductive receptacles, with male receptacles developing earlier than female ones during spring (Figures 1A, 1B, and 4A–4F).[28,33] This implies that the molecular machineries essential for both male and female sexual reproduction must be functional in each *M. quadrata* individual. Sex in the dioicous *M. polymorpha* is determined by the dominant U-linked *Feminizer* (*BPCU*) gene (Figure S3).[22] *BPCU* represses the transcription of the long non-coding RNA *SUF*, thereby enabling expression of the autosomal *FGMYB* gene, which promotes feminization.[22,23] In the absence of *BPCU* (e.g., in males), *SUF* transcription represses the expression of the *FGMYB* gene, resulting in male plants.[23,24] On the other hand, *BPCV* (the V-linked gametolog of *BPCU*) is not involved in sex determination, but both *BPCU* and *BPCV* play essential roles in the induction of sexual reproduction.[22] If the regulation of sexual reproduction is conserved between the dioicous *M. polymorpha* and the monoicous *M. quadrata*, we expect major regulators to be present and fully functional in each individual of the cosexual species. We found two *BPCU* and one *BPCV* orthologs in *M. quadrata* (Figure S4; Table S4). While *BPCV* resides on chromosome 9, *BPCU* was translocated to chromosome 4 together with the homolog of a U-specific gene (MpUg00040), and both were duplicated so that they now occur in an inverted repeat (Figure S4). The paucity of substitutions between the two copies of these two gene pairs implies a young duplication age. We also found one homolog of *FGMYB* that has, on its antisense strand, a sequence similar to the regulatory regions of *SUF* in *M. polymorpha*.[24] However, the transcript region is only partially conserved (Figure S5). *FGMYB* and its putative *cis* repressor (*SUF*) both occur on chromosome 1, as in the dioicous *M. polymorpha*,[23] implying that its genomic position did not change during the transition to monoicy. Taken together, our data suggest that the translocation of *BPCU* to

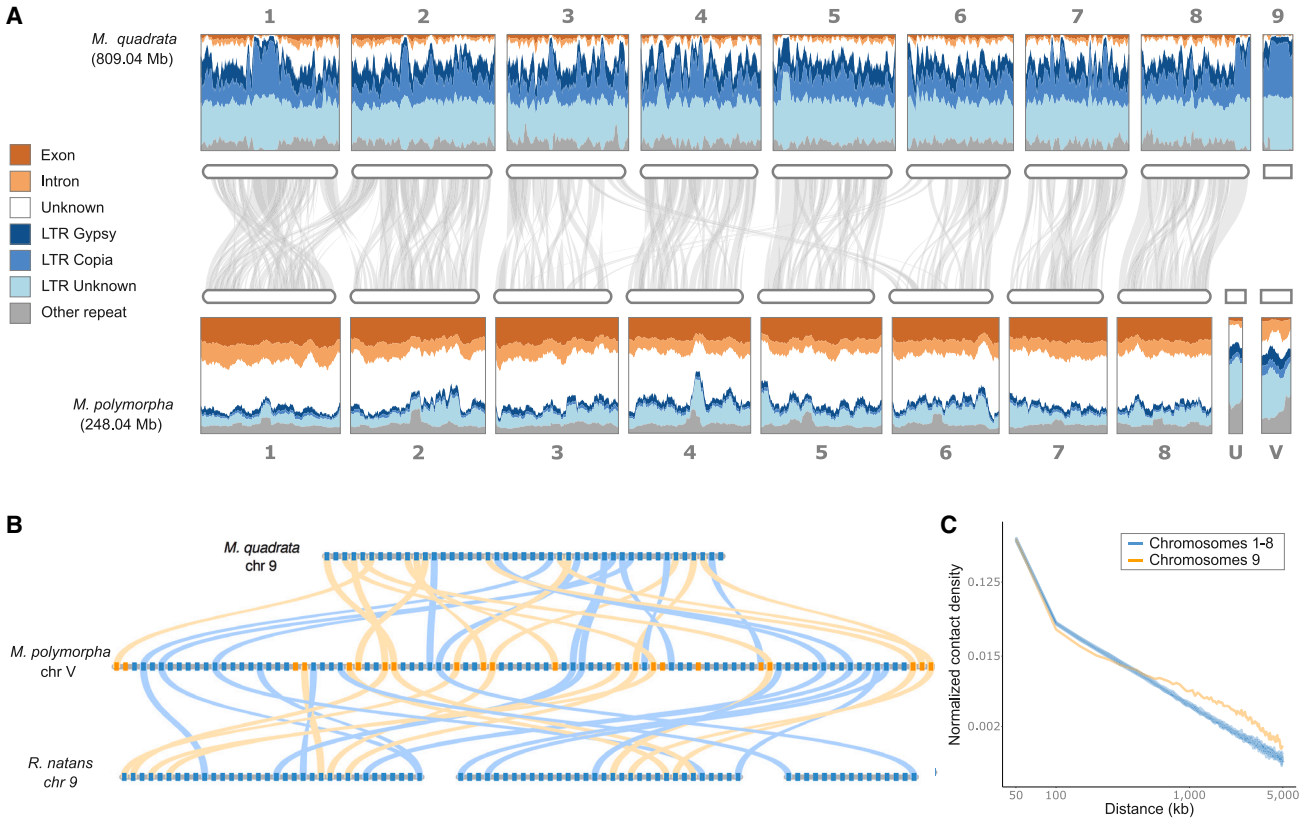

Figure 3. Chromosome nine of *M. quadrata* is homologous to the V chromosome of *M. polymorpha*

(A) Collinearity (gray ribbons connect syntenic blocks of ≥3 genes), repeat, and gene density of the monoicous *M. quadrata* and the dioicous *M. polymorpha* genomes estimated in 2 Mb sliding windows (500 kb steps).

(B) Microsynteny plot of *M. polymorpha* chromosome V and chromosome nine of *M. quadrata* and *R. natans*. Blue and orange dots represent V-specific genes and gametologs of *M. polymorpha*, respectively. Ribbons connect homologs and use the same color code.

(C) Intra-chromosomal interaction decay within chromosomes of *M. quadrata*.

an autosome was critical for making the molecular machinery of male and female sexual reproduction accessible in each individual, thus achieving monoicy.

Altered regulation of the *Feminizer* gene enables combined expression of conserved male and female reproductive programs

To test whether the molecular machinery that determines sex in the dioicous *M. polymorpha* has retained its function in the monoicous *M. quadrata*, we compared the expression levels of *BPCU*, *BPCV*, *FGMYB*, and *SUF* across different tissues. While *BPCU* was strongly expressed in the female reproductive receptacles and barely detectable in male receptacles, *BPCV* showed nearly identical expression levels in both male and female receptacles (Figures 4G and 4H). Furthermore, *FGMYB* expression was significantly higher in female than in male receptacles, while high levels of antisense transcripts (*SUF*) were detected in male receptacles (Figures 4I–4K). These observations mirror the regulation of the *FGMYB-SUF* module in the dioicous *M. polymorpha*, indicating functional conservation.[22–24] They further imply that *BPCU*[22] acquired new regulatory mechanisms enabling the expression of both male and female functions in a single individual (Figure 4L).

Shared genomic changes between *M. polymorpha* and *R. natans* in the transition to cosexuality

Despite the identification of the main sex-determining genes in *M. polymorpha*, evidence from reverse genetic experiments indicates that sex chromosomes carry genes (other than the sex-determining gene *BPCU*) that are essential for the differentiation of functional male and female gametes.[22,23] Specifically, mutants carrying the V chromosome but exhibiting the female phenotype (e.g., *suf* mutant and male wild type with introduced *BPCU* gene) fail to form egg cells,[22,23] while mutants carrying the U chromosome but exhibiting the male phenotype (e.g., *fgmyb* mutants) produce immotile sperm.[23] Since both *M. quadrata* and *R. natans* have likely retained the molecular machinery required to produce both male and female sexual organs and gametes, they are also expected to have preserved the essential genes necessary to their development.

Homologs of *M. polymorpha* U- and V-specific genes retained in *R. natans* and *M. quadrata* were highly overlapping (Table S4), with multiple V-specific but only one U-specific gene homologs being conserved when using the latest version of the *M. polymorpha* genome, v.7.1 (https://marchantia.info). This implies that these homologs may be essential to male and female

CellPress
OPEN ACCESS

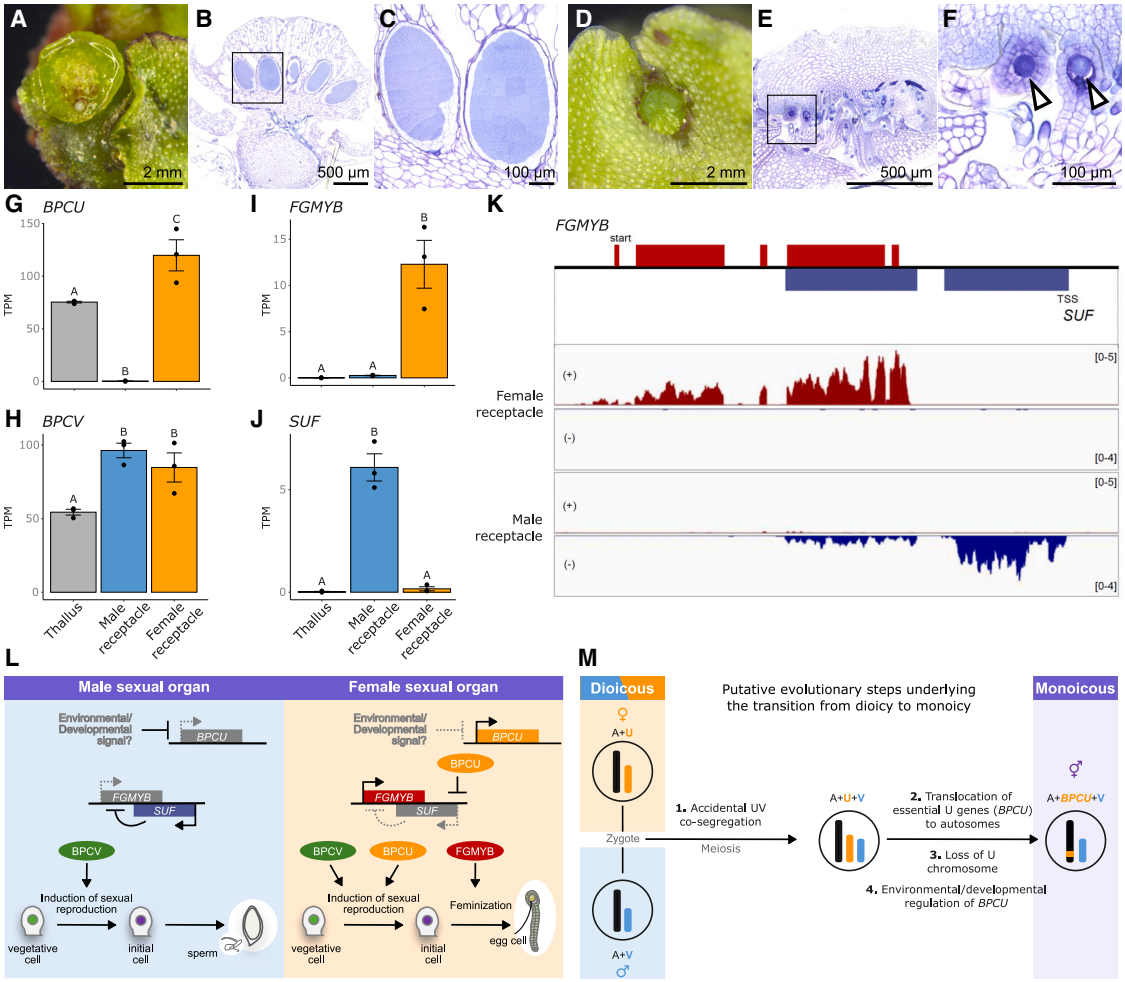

Figure 4. Evolutionary changes underlying the transition from dioicy to monoicy

(A–F) Male (A–C) and female (D–F) sexual receptacles (A, B, D, and E) and sexual organs (C and F) formed on *M. quadrata*. (C and F) Close-ups of the framed regions in (B) and (E), respectively. Arrowheads indicate egg cells.

(G–K) Expression levels of (G) *BPCU*, (H) *BPCV*, (I) *FGMYB*, and (J) *SUF* homologs in thallus, male receptacles, and female receptacles of *M. quadrata*. Bars represent the mean ± SE. Symbols above the bars indicate grouping by $p < 0.05$ in a Tukey-Kramer test ($n = 3$).

(K) Read accumulation at *FGMYB-SUF* loci in female and male receptacles. Read coverage on the sense (+) and antisense (−) strands are shown separately, and the numbers in brackets indicate bins per million mapped reads.

(L) Proposed model for the regulation of sexual differentiation in *M. quadrata*: in male receptacles, *BPCU* expression is suppressed; in female receptacles, *BPCU* might promote the expression of *FGMYB* gene as in *M. polymorpha*. Since *BPCV* is likely required for the induction of reproductive organs, *M. quadrata* possesses both *BPCU* and *BPCV*.

(M) Putative evolutionary changes underlying the transition from dioicy to monoicy during the evolution of *M. quadrata*.

reproductive functions, respectively. On the other hand, there was no consistency between *R. natans* and *M. quadrata* regarding which gametolog alleles were retained (Table S4; Figure S2). The *BPCU/V* gene was the only gametolog for which both alleles were retained in both species, in line with the finding that they are necessary for inducing female and male sexual reproductive organs, respectively.[22] Our findings suggest that there were only two essential genes on the U chromosome (*BPCU* and MpUg00040), and this may explain the preferential retention of the V and loss of the U chromosome in the transition to monoicy both in *M. quadrata* and *R. natans* (Figure 4M). While details of the mating system transition remain to be revealed (Figures 4L and 4M), retention of highly overlapping homologous V- and U-linked gene sets in the two monoicous liverwort species suggests that it is driven by functional constraints.

Conclusions

The results observed in *M. quadrata* and those previously found in *R. natans*[21] reveal surprisingly similar evolutionary trajectories in the transition to monoicy in the two species, namely the preferential retention of the V-linked and loss of most U-linked genes. We ascribe this remarkable molecular convergence to two factors. First, natural selection disfavored the co-occurrence of U and V sex chromosomes to minimize their sexually

antagonistic effects while simultaneously enabling male and female sexual functions in each individual, as predicted by theory.[13,18,19] Second, the V chromosome potentially contains more genes essential to produce sexual organs and gametangia than the U chromosome, supported by the observation that a vastly greater number of V-linked than U-linked genes was retained in both *M. quadrata* and *R. natans*. Furthermore, expression analysis in *M. quadrata* indicates the functional conservation of genes involved in sex determination and differentiation during the transition from dioicy to monoicy, as well as the acquisition of environmental or developmental regulation of the *Feminizer* gene (*BPCU*), which allows the production of both male and female reproductive structures in the same individual. We speculate that the duplication and translocation of the *BPCU* gene may have been crucial for achieving monoicy through the expression of both male and female functions in a single genetic individual.

Does this remarkable molecular convergence extend to other liverworts and eukaryotes possessing U/V sex chromosomes? Intriguingly, some evidence suggests preferential retention of V-linked over U-linked genes in monoicous species of green and brown algae and mosses.[14,15,20] Because these organisms all possess haploid U/V sex chromosomes, haploidy may be the primary evolutionary force driving convergence. If this speculation turned out to be true, it would represent one of the most remarkable examples of convergent evolution spanning multiple major eukaryotic lineages. Furthermore, revealing convergent and divergent evolutionary changes associated with the dioicy-to-monoicy transition in different groups of eukaryotes with U/V sex chromosomes would help us to better understand the ultimate forces, such as the role of additive vs. epistatic effects, driving sex chromosome evolution in general.[18,19]

Limitations of the study

Our study characterized the molecular basis of the transition to cosexuality in the liverwort *M. quadrata* and identified an evolutionary trajectory strikingly similar to that observed in another species, *R. natans*.[21] However, two main questions remain unanswered. First, although we have shown that the key sex-determining molecular machinery is conserved between *M. quadrata* and its dioicous relative *M. polymorpha*, it is still unknown which environmental or developmental factors (or a combination thereof) regulate the independent formation of male and female sex organs. Second, the observed convergence is based on only two species, making it difficult to generalize our findings to liverworts or eukaryotes more broadly. Future studies should address these limitations by, for example, testing the formation of male vs. female sexual structures under different environmental conditions and extending our analyses to a wider range of species that have undergone independent transitions to cosexuality.

RESOURCE AVAILABILITY

Lead contact

More information or resource requests should be forwarded to the lead contact, Péter Szövényi (peter.szoevenyi@uzh.ch).

Materials availability

This study did not generate new unique reagents.

Data and code availability

- This paper does not report original code.
- The raw PacBio HiFi, Illumina DNA sequencing (DNA-seq), and Omni-C reads, as well as Illumina RNA-seq and Iso-seq data are deposited in NCBI SRA under the BioProject number PRJNA1159831 (SRA: PRJNA1159831) and in DDBJ under the BioProject number PRJDB18811 (DDBJ: PRJDB18811).
- Assembly and annotation of the *M. quadrata* genome are available in Figshare (https://doi.org/10.6084/m9.figshare.27055057) and will also be released on Phytozome upon publication (https://phytozome-next.jgi.doe.gov/ogg/). Assemblies of the *M. quadrata* organelle genomes are deposited in DDBJ under the accession numbers LC853331–LC853332 (DDBJ: LC853331, LC853332).

ACKNOWLEDGMENTS

The work (proposal: 10.46936/10.25585/60001405) conducted by the US Department of Energy Joint Genome Institute (https://ror.org/04xm1d337), a DOE Office of Science User Facility, is supported by the Office of Science of the US Department of Energy operated under contract no. DE-AC02-05CH11231. This research received further financial support from the URPP Evolution in Action of the University of Zurich, the Swiss National Science Foundation (grant nos. 131726, 160004, 184826, and 212509), the EU's Horizon 2020 Research and Innovation Program (PlantHUB-No. 722338), the Georges and Antoine Claraz Foundation, and the Forschgungskredit of the University of Zurich (FK-20-089) to P.S. It was also supported by the Japan Society for the Promotion of Science (JSPS) KAKENHI Grant-in-Aid for Scientific Research (C) (21K06228 to Y.Y.), a Grant-in-Aid for Transformative Research Areas (22H05172 and 23H04744 to Y.Y.), the JST FOREST Program (JPMJFR2256 to Y.Y.), the JSPS KAKENHI Grant-in-Aid for Scientific Research (A) (22H00417 to T.K.), the Fund for Promotion of Joint International Research (22K21352 to T.K.), and a Grant-in-Aid for Challenging Research (22K19345 to T.K.). This work was also supported by the NIBB Collaborative Research Program (23NIBB441 and 24NIBB428 to Y.Y.) and the research priority program MAdLand (https://madland.science, DFG priority program 2237, PS-1111/1 to P.S.). We thank Chikako Inoue for providing technical assistance with plant observations as well as Yasuhiro Tanizawa for making the *M. polymorpha* v.7.1 genome (MarpolBase, https://marchantia.info/) available for comparative analysis and for providing permission to use it in this study. We thank Yoshihiro Yoshitake and Yukari Sando (NGS core facility of the Graduate Schools of Biostudies, Kyoto University) for supporting RNA sequencing for gene annotation and expression. Computation time was partly provided by the Super Computer System, Institute for Chemical Research, Kyoto University.

AUTHOR CONTRIBUTIONS

Y.Y., T.K., and P.S. conceptualized the project, coordinated the research, and wrote the manuscript. E.S., G.P., J.J., R.N.W., K.Y., and S.S. carried out bioinformatic analyses. Sequencing and library preparation were done by J.G., N.K., and R.L. and coordinated by J.S. and J.L.-M. G.P., E.S., S.K., S.Z., T.B., and K.T.Y. performed genome annotation, and G.P., Y.Y., and Y.U. performed the phylogenetic analysis. Y.Y., E.S., and T.T. carried out RNA-sequencing analysis for gene expression. Y.Y. conducted histological observations. M.S. collected the *M. quadrata* plant from its natural habitat. All authors have revised and approved the final version of the manuscript.

DECLARATION OF INTERESTS

The authors declare no competing interests.

STAR★METHODS

Detailed methods are provided in the online version of this paper and include the following:

- KEY RESOURCES TABLE
- EXPERIMENTAL MODEL AND STUDY PARTICIPANT DETAILS

SUPPLEMENTAL INFORMATION

Supplemental information can be found online at https://doi.org/10.1016/j.celrep.2025.115503.

Received: December 12, 2024
Revised: February 13, 2025
Accepted: March 11, 2025

REFERENCES

1. Cronk, Q. (2022). The distribution of sexual function in the flowering plant: from monoecy to dioecy. Philos. Trans. R. Soc. Lond. B Biol. Sci. *377*, 20210486. https://doi.org/10.1098/rstb.2021.0486.
2. Cutter, A.D. (2019). Reproductive transitions in plants and animals: selfing syndrome, sexual selection and speciation. New. Phytol. *224*, 1080–1094. https://doi.org/10.1111/nph.16075.
3. Pannell, J.R., and Jordan, C.Y. (2022). Evolutionary Transitions Between Hermaphroditism and Dioecy in Animals and Plants. Annu. Rev. Ecol. Evol. Syst. *53*, 183–201. https://doi.org/10.1146/annurev-ecolsys-102320-085812.
4. Cossard, G.G., Gerchen, J.F., Li, X., Cuenot, Y., and Pannell, J.R. (2021). The rapid dissolution of dioecy by experimental evolution. Curr. Biol. *31*, 1277–1283.e5. https://doi.org/10.1016/j.cub.2020.12.028.
5. Käfer, J., Marais, G.A.B., and Pannell, J.R. (2017). On the rarity of dioecy in flowering plants. Mol. Ecol. *26*, 1225–1241. https://doi.org/10.1111/mec.14020.
6. Käfer, J., Méndez, M., and Mousset, S. (2022). Labile sex expression in angiosperm species with sex chromosomes. Philos. Trans. R. Soc. B Biol. Sci. *377*. https://doi.org/10.1098/rstb.2021.0216.
7. Saunders, P.A., and Muyle, A. (2024). Sex Chromosome Evolution: Hallmarks and Question Marks. Mol. Biol. Evol. *41*, msae218. https://doi.org/10.1093/molbev/msae218.
8. Bachtrog, D., Mank, J.E., Peichel, C.L., Kirkpatrick, M., Otto, S.P., Ashman, T.-L., Hahn, M.W., Kitano, J., Mayrose, I., Ming, R., et al. (2014). Sex determination: why so many ways of doing it? PLoS Biol. *12*, e1001899. https://doi.org/10.1371/journal.pbio.1001899.
9. Wright, A.E., Dean, R., Zimmer, F., and Mank, J.E. (2016). How to make a sex chromosome. Nat. Commun. *7*, 12087. https://doi.org/10.1038/ncomms12087.
10. Bergero, R., and Charlesworth, D. (2009). The evolution of restricted recombination in sex chromosomes. Trends Ecol. Evol. *24*, 94–102. https://doi.org/10.1016/j.tree.2008.09.010.
11. Rice, W.R. (1984). Sex Chromosomes and the Evolution of Sexual Dimorphism. Evolution *38*, 735–742. https://doi.org/10.2307/2408385.
12. Frank, S.A., and Patten, M.M. (2020). Sexual antagonism leads to a mosaic of X-autosome conflict. Evolution *74*, 495–498. https://doi.org/10.1111/evo.13918.
13. Gibson, J.R., Chippindale, A.K., and Rice, W.R. (2002). The X chromosome is a hot spot for sexually antagonistic fitness variation. Proc. Biol. Sci. *269*, 499–505. https://doi.org/10.1098/rspb.2001.1863.
14. Healey, A.L., Piatkowski, B., Lovell, J.T., Sreedasyam, A., Carey, S.B., Mamidi, S., Shu, S., Plott, C., Jenkins, J., Lawrence, T., et al. (2023). Newly identified sex chromosomes in the Sphagnum (peat moss) genome alter carbon sequestration and ecosystem dynamics. Nat. Plants *9*, 238–254. https://doi.org/10.1038/s41477-022-01333-5.
15. Barrera-Redondo, J., Lipinska, A.P., Liu, P., Dinatale, E., Cossard, G., Godfroy, O., Heesch, S., Nehr, Z., Brillet-Guéguen, L., Peters, A.F., et al. (2024). Origin and evolutionary trajectories of brown algal sex chromosomes. Preprint at bioRxiv. https://doi.org/10.1101/2024.01.15.575685.
16. Immler, S., Arnqvist, G., and Otto, S.P. (2012). Ploidally antagonistic selection maintains stable genetic polymorphism. Evolution *66*, 55–65. https://doi.org/10.1111/j.1558-5646.2011.01399.x.
17. Coelho, S.M., Gueno, J., Lipinska, A.P., Cock, J.M., and Umen, J.G. (2018). UV Chromosomes and Haploid Sexual Systems. Trends. Plant. Sci. *23*, 794–807. https://doi.org/10.1016/j.tplants.2018.06.005.
18. McDaniel, S.F. (2023). Divergent outcomes of genetic conflict on the UV sex chromosomes of Marchantia polymorpha and Ceratodon purpureus. Curr. Opin. Genet. Dev. *83*, 102129. https://doi.org/10.1016/j.gde.2023.102129.
19. Carey, S.B., Kollar, L.M., and McDaniel, S.F. (2021). Does degeneration or genetic conflict shape gene content on UV sex chromosomes? Bryophyt. Divers. Evol. *43*. https://doi.org/10.11646/bde.43.1.11.
20. Takahashi, K., Suzuki, S., Kawai-Toyooka, H., Yamamoto, K., Hamaji, T., Ootsuki, R., Yamaguchi, H., Kawachi, M., Higashiyama, T., and Nozaki, H. (2023). Reorganization of the ancestral sex-determining regions during the evolution of trioecy in Pleodorina starrii. Commun. Biol. *6*, 590. https://doi.org/10.1038/s42003-023-04949-1.
21. Singh, S., Davies, K.M., Chagné, D., and Bowman, J.L. (2023). The fate of sex chromosomes during the evolution of monoicy from dioicy in liverworts. Curr. Biol. *33*, 3597–3609. https://doi.org/10.1016/j.cub.2023.07.023.
22. Iwasaki, M., Kajiwara, T., Yasui, Y., Yoshitake, Y., Miyazaki, M., Kawamura, S., Suetsugu, N., Nishihama, R., Yamaoka, S., Wanke, D., et al. (2021). Identification of the sex-determining factor in the liverwort Marchantia polymorpha reveals unique evolution of sex chromosomes in a haploid system. Curr. Biol. *31*, 5522–5532.e7. https://doi.org/10.1016/j.cub.2021.10.023.
23. Hisanaga, T., Okahashi, K., Yamaoka, S., Kajiwara, T., Nishihama, R., Shimamura, M., Yamato, K.T., Bowman, J.L., Kohchi, T., and Nakajima, K. (2019). A cis-acting bidirectional transcription switch controls sexual dimorphism in the liverwort. EMBO J. *38*, e100240. https://doi.org/10.15252/embj.2018100240.
24. Kajiwara, T., Miyazaki, M., Yamaoka, S., Yoshitake, Y., Yasui, Y., Nishihama, R., and Kohchi, T. (2024). Transcription of the Antisense Long Non-Coding RNA, SUPPRESSOR OF FEMINIZATION, Represses Expression of the Female-Promoting Gene FEMALE GAMETOPHYTE MYB in the Liverwort Marchantia polymorpha. Plant. Cell. Physiol. *65*, 338–349. https://doi.org/10.1093/pcp/pcad170.
25. Berrie, G.K. (1963). Cytology and Phylogeny of Liverworts. Evolution *17*, 347. https://doi.org/10.2307/2406164.
26. Yamato, K.T., Ishizaki, K., Fujisawa, M., Okada, S., Nakayama, S., Fujishita, M., Bando, H., Yodoya, K., Hayashi, K., Bando, T., et al. (2007). Gene organization of the liverwort Y chromosome reveals distinct sex chromosome evolution in a haploid system. Proc. Natl. Acad. Sci. USA *104*, 6472–6477. https://doi.org/10.1073/pnas.0609054104.
27. Laenen, B., Machac, A., Gradstein, S.R., Shaw, B., Patiño, J., Désamoré, A., Goffinet, B., Cox, C.J., Shaw, A.J., and Vanderpoorten, A. (2016). Increased diversification rates follow shifts to bisexuality in liverworts. New Phytol. *210*, 1121–1129. https://doi.org/10.1111/nph.13835.
28. Haupt, A.W. (1926). Morphology of Preissia quadrata. Bot. Gaz. *82*, 30–54.
29. Villarreal A, J.C., Crandall-Stotler, B.J., Hart, M.L., Long, D.G., and Forrest, L.L. (2015). Divergence times and the evolution of morphological complexity in an early land plant lineage (Marchantiopsida) with a slow molecular rate. New Phytol. *209*, 1734–1746. https://doi.org/10.1111/nph.13716.

30. Bowman, J.L., Kohchi, T., Yamato, K.T., Jenkins, J., Shu, S., Ishizaki, K., Yamaoka, S., Nishihama, R., Nakamura, Y., Berger, F., et al. (2017). Insights into Land Plant Evolution Garnered from the Marchantia polymorpha Genome. Cell *171*, 287–304.e15. https://doi.org/10.1016/j.cell.2017.09.030.

31. Montgomery, S.A., Tanizawa, Y., Galik, B., Wang, N., Ito, T., Mochizuki, T., Akimcheva, S., Bowman, J.L., Cognat, V., Maréchal-Drouard, L., et al. (2020). Chromatin Organization in Early Land Plants Reveals an Ancestral Association between H3K27me3, Transposons, and Constitutive Heterochromatin. Curr. Biol. *30*, 573–588.e7. https://doi.org/10.1016/j.cub.2019.12.015.

32. Kohchi, T., Yamato, K.T., Ishizaki, K., Yamaoka, S., and Nishihama, R. (2021). Development and Molecular Genetics of Marchantia polymorpha. Annu. Rev. Plant Biol. *72*, 677–702. https://doi.org/10.1146/annurev-arplant-082520-094256.

33. Xiao, Y., and Shimamura, M. (2024). Morphological and phenological studies on sexual reproduction of Preissia quadrata (Marchantiaceae, Marchantiophyta). Hikobia *19*, 75–85.

34. Gamborg, O.L., Miller, R.A., and Ojima, K. (1968). Nutrient requirements of suspension cultures of soybean root cells. Exp. Cell. Res. *50*, 151–158. https://doi.org/10.1016/0014-4827(68)90403-5.

35. Cove, D.J., Perroud, P., Charron, A.J., McDaniel, S.F., Khandelwal, A., and Quatrano, R.S. (2009). Culturing the moss Physcomitrella patens. Cold Spring Harb. Protoc. *2009*, pdb.prot5136.

36. Porebski, S., Bailey, L.G., and Baum, B.R. (1997). Modification of a CTAB DNA extraction protocol for plants containing high polysaccharide and polyphenol components. Plant. Mol. Biol. Rep. *15*, 8–15. https://doi.org/10.1007/BF02772108.

37. Cheng, H., Concepcion, G.T., Feng, X., Zhang, H., and Li, H. (2021). Haplotype-resolved de novo assembly using phased assembly graphs with hifiasm. Nat. Methods *18*, 170–175. https://doi.org/10.1038/s41592-020-01056-5.

38. Cheng, H., Jarvis, E.D., Fedrigo, O., Koepfli, K.-P., Urban, L., Gemmell, N.J., and Li, H. (2022). Haplotype-resolved assembly of diploid genomes without parental data. Nat. Biotechnol. *40*, 1332–1335. https://doi.org/10.1038/s41587-022-01261-x.

39. Vaser, R., Sović, I., Nagarajan, N., and Šikić, M. (2017). Fast and accurate de novo genome assembly from long uncorrected reads. Genome Res. *27*, 737–746. https://doi.org/10.1101/gr.214270.116.

40. Durand, N.C., Shamim, M.S., Machol, I., Rao, S.S.P., Huntley, M.H., Lander, E.S., and Aiden, E.L. (2016). Juicer Provides a One-Click System for Analyzing Loop-Resolution Hi-C Experiments. Cell Syst. *3*, 95–98. https://doi.org/10.1016/j.cels.2016.07.002.

41. Manni, M., Berkeley, M.R., Seppey, M., and Zdobnov, E.M. (2021). BUSCO: Assessing Genomic Data Quality and Beyond. Curr. Protoc. *1*, e323. https://doi.org/10.1002/cpz1.323.

42. Mokhtar, M.M., Abd-Elhalim, H.M., and El Allali, A. (2023). A large-scale assessment of the quality of plant genome assemblies using the LTR assembly index. AoB Plants *15*, plad015. https://doi.org/10.1093/aobpla/plad015.

43. Ou, S., and Jiang, N. (2018). LTR_retriever: A highly accurate and sensitive program for identification of long terminal repeat retrotransposons. Plant. Physiol. *176*, 1410–1422. https://doi.org/10.1104/pp.17.01310.

44. Jin, J.-J., Yu, W.-B., Yang, J.-B., Song, Y., DePamphilis, C.W., Yi, T.-S., and Li, D.-Z. (2020). GetOrganelle: a fast and versatile toolkit for accurate de novo assembly of organelle genomes. Genome. Biol. *21*, 241. https://doi.org/10.1186/s13059-020-02154-5.

45. Li, H. (2018). Minimap2: pairwise alignment for nucleotide sequences. Bioinformatics *34*, 3094–3100. https://doi.org/10.1093/bioinformatics/bty191.

46. Tillich, M., Lehwark, P., Pellizzer, T., Ulbricht-Jones, E.S., Fischer, A., Bock, R., and Greiner, S. (2017). GeSeq - versatile and accurate annotation of organelle genomes. Nucleic. Acids. Res. *45*, W6–W11. https://doi.org/10.1093/nar/gkx391.

47. Greiner, S., Lehwark, P., and Bock, R. (2019). OrganellarGenomeDRAW (OGDRAW) version 1.3.1: expanded toolkit for the graphical visualization of organellar genomes. Nucleic Acids Res. *47*, W59–W64. https://doi.org/10.1093/nar/gkz238.

48. Kent, W.J. (2002). BLAT - The BLAST-like alignment tool. Genome. Res. *12*, 656–664. https://doi.org/10.1101/gr.229202.

49. Laslett, D., and Canback, B. (2004). ARAGORN, a program to detect tRNA genes and tmRNA genes in nucleotide sequences. Nucleic Acids Res. *32*, 11–16. https://doi.org/10.1093/nar/gkh152.

50. Gabriel, L., Brůna, T., Hoff, K.J., Ebel, M., Lomsadze, A., Borodovsky, M., and Stanke, M. (2024). BRAKER3: Fully automated genome annotation using RNA-seq and protein evidence with GeneMark-ETP, AUGUSTUS and TSEBRA. Preprint at bioRxiv. https://doi.org/10.1101/2023.06.10.544449.

51. Flynn, J.M., Hubley, R., Goubert, C., Rosen, J., Clark, A.G., Feschotte, C., and Smit, A.F. (2020). RepeatModeler2 for automated genomic discovery of transposable element families. Proc. Natl. Acad. Sci. USA *117*, 9451–9457. https://doi.org/10.1073/pnas.1921046117.

52. Kapitonov, V.V., and Jurka, J. (2008). A universal classification of eukaryotic transposable elements implemented in Repbase. Nat. Rev. Genet. *9*, 411–414. https://doi.org/10.1038/nrg2165-c1.

53. Smit, A., Hubley, R., and Green, P. (2015). RepeatMasker Open-4.0. https://www.repeatmasker.org/

54. Pertea, M., Kim, D., Pertea, G.M., Leek, J.T., and Salzberg, S.L. (2016). Transcript-level expression analysis of RNA-seq experiments with HISAT, StringTie and Ballgown. Nat. Protoc. *11*, 1650–1667. https://doi.org/10.1038/nprot.2016.095.

55. Ou, S., Su, W., Liao, Y., Chougule, K., Agda, J.R.A., Hellinga, A.J., Lugo, C.S.B., Elliott, T.A., Ware, D., Peterson, T., et al. (2019). Benchmarking transposable element annotation methods for creation of a streamlined, comprehensive pipeline. Genome Biol. *20*, 275. https://doi.org/10.1186/s13059-019-1905-y.

56. Linde, A.-M., Singh, S., Bowman, J.L., Eklund, M., Cronberg, N., and Lagercrantz, U. (2023). Genome Evolution in Plants: Complex Thalloid Liverworts (Marchantiopsida). Genome Biol. Evol. *15*, evad014–10. https://doi.org/10.1093/gbe/evad014.

57. Emms, D.M., and Kelly, S. (2019). OrthoFinder: phylogenetic orthology inference for comparative genomics. Genome Biol. *20*, 238. https://doi.org/10.1186/s13059-019-1832-y.

58. Edgar, R.C. (2004). MUSCLE: Multiple sequence alignment with high accuracy and high throughput. Nucleic Acids Res. *32*, 1792–1797. https://doi.org/10.1093/nar/gkh340.

59. Minh, B.Q., Schmidt, H.A., Chernomor, O., Schrempf, D., Woodhams, M.D., von Haeseler, A., and Lanfear, R. (2020). IQ-TREE 2: New Models and Efficient Methods for Phylogenetic Inference in the Genomic Era. Mol. Biol. Evol. *37*, 1530–1534. https://doi.org/10.1093/molbev/msaa015.

60. Wang, Y., Tang, H., Debarry, J.D., Tan, X., Li, J., Wang, X., Lee, T.H., Jin, H., Marler, B., Guo, H., et al. (2012). MCScanX: A toolkit for detection and evolutionary analysis of gene synteny and collinearity. Nucleic Acids Res. *40*, e49. https://doi.org/10.1093/nar/gkr1293.

61. Ewels, P.A., Peltzer, A., Fillinger, S., Patel, H., Alneberg, J., Wilm, A., Garcia, M.U., Di Tommaso, P., and Nahnsen, S. (2020). The nf-core framework for community-curated bioinformatics pipelines. Nat. Biotechnol. *38*, 276–278. https://doi.org/10.1038/s41587-020-0439-x.

62. Ramírez, F., Ryan, D.P., Grüning, B., Bhardwaj, V., Kilpert, F., Richter, A.S., Heyne, S., Dündar, F., and Manke, T. (2016). deepTools2: a next generation web server for deep-sequencing data analysis. Nucleic Acids Res. *44*, W160–W165. https://doi.org/10.1093/nar/gkw257.

63. Liao, Y., Smyth, G.K., and Shi, W. (2014). featureCounts: an efficient general purpose program for assigning sequence reads to genomic

features. Bioinformatics *30*, 923–930. https://doi.org/10.1093/bioinformatics/btt656.

64. R Core Team (2022). R: A Language and Environment for Statistical Computing (R Foundation for Statistical Computing).

65. Vasimuddin, M., Misra, S., Li, H., and Aluru, S. (2019). Efficient Architecture-Aware Acceleration of BWA-MEM for Multicore Systems. In 2019 IEEE International Parallel and Distributed Processing Symposium (IPDPS) (IEEE), pp. 314–324. https://doi.org/10.1109/IPDPS.2019.00041.

66. Open2C; Abdennur, N., Fudenberg, G., Flyamer, I.M., Galitsyna, A.A., Goloborodko, A., Imakaev, M., and Venev, S.V. (2023). Pairtools: from sequencing data to chromosome contacts. Preprint at bioRxiv. https://doi.org/10.1101/2023.02.13.528389.

STAR★METHODS

KEY RESOURCES TABLE

REAGENT or RESOURCE	SOURCE	IDENTIFIER
Biological samples		
Marchantia quadrata	Mt Kitadake in Minami Alps city, Japan	isolate Kitadake-1
Chemicals, peptides, and recombinant proteins		
Cetyltrimethylammonium bromide (CTAB)	Millipore Sigma	CCAS 57-09-0
Plant Agar	Millipore Sigma	CCAS 39346-81-1
Gamborg′s B-5 Basal Medium with Minimal Organics	Millipore Sigma	Cat#12352207
RNA*later* Stabilization Solution	Thermo Fisher	Cat#AM7021
TRIzol reagent	Thermo Fisher	Cat#15596026
DNase I, RNase-free	Thermo Fisher	Cat#EN0521
Formaldehyde solution	Millipore Sigma	Cat#50-00-0
Ethanol	Millipore Sigma	Cat#200-578-6
Acetic acid solution	Millipore Sigma	CCAS 64-19-7
Technovit 7100	Heraeus Kulzer	N/A
Toluidine Blue	Millipore Sigma	CCAS 6586-04-5
Deposited data		
Raw DNA- and RNA-seq data used to assemble and annotate the *M. quadrata* genome	NCBI SRA and DDBJ	SRA: PRJNA1159831 and DDBJ: PRJDB18811
Genome assembly and annotation of M. quadrata genome	Figshare and Phytozome	https://doi.org/10.6084/m9.figshare.27055057; https://phytozome-next.jgi.doe.gov/ogg/
M. quadrata organelle genomes	DDBJ	DDBJ: LC853331, LC853332
Software and algorithms		
HiFiAsm 0.19.5-r587	https://github.com/chhylp123/hifiasm	N/A
RACON v1.4.3	https://github.com/isovic/racon	N/A
JUICER pipeline v1.6	https://github.com/aidenlab/juicer	N/A
Marchantia polymorpha v7. genome	https://marchantia.info/data/MpTak_v7.1_standard_genome/	N/A
BUSCO v5.6.1	https://busco.ezlab.org/busco_userguide.html	N/A
LTR_retriever v2.9.0	https://github.com/oushujun/LTR_retriever	N/A
GetOrganelle v1.7.7.0	https://github.com/Kinggerm/GetOrganelle	N/A
SnapGene v7.2.1	https://www.snapgene.com/updates/snapgene-version-7-2-1	N/A
Minimap2 v2.28-r1209	https://github.com/lh3/minimap2/releases?after=v2.5	N/A
GeSeq v2.03	https://chlorobox.mpimp-golm.mpg.de/geseq.html	N/A
OGDRAW v1.3.1	https://chlorobox.mpimp-golm.mpg.de/OGDraw.html	N/A
BLAT v35.1	https://github.com/djhshih/blat	N/A
HMMER v3.4	http://hmmer.org/	N/A
ARAGORN v1.2.38	https://www.trna.se/	N/A
Braker v3.0.1	https://github.com/Gaius-Augustus/BRAKER/releases	N/A
OrthoDB 10	www.orthodb.org	N/A

(*Continued on next page*)

Continued

REAGENT or RESOURCE	SOURCE	IDENTIFIER
RepeatModeler v2.0.3	https://github.com/Dfam-consortium/RepeatModeler/releases	N/A
RepBase	https://www.girinst.org/repbase/	N/A
RepeatMasker v4.0.9	https://www.repeatmasker.org/	N/A
HISAT v2.1.0	https://daehwankimlab.github.io/hisat2/download/	N/A
TSEBRA v1.1.2.5	https://github.com/Gaius-Augustus/TSEBRA	N/A
Extensive *De novo* TE Annotator (EDTA) v1.9.2	https://github.com/oushujun/EDTA	N/A
OrthoFinder v2.3.11	https://github.com/davidemms/OrthoFinder/releases	N/A
muscle v5.2	https://www.drive5.com/muscle5/	N/A
IQ-TREE v2.0.6	https://archive.org/details/iqtree-2.0.6	N/A
MCScan	https://github.com/tanghaibao/jcvi/wiki/MCscan-%28Python-version%29	N/A
nfcore/rnaseq pipeline v3.13.2	https://github.com/nf-core/RNAseq/releases	N/A
DeepTools v3.5.6	https://github.com/deeptools/deepTools	N/A
FeatureCounts v2.18.0	https://subread.sourceforge.net/featureCounts.html	N/A
R v4.1.0	https://www.r-project.org/	N/A
BWA mem2 v2.2.1	https://github.com/bwa-mem2/bwa-mem2/releases	N/A
pairtools v0.3.0	https://github.com/open2c/pairtools/releases	N/A

EXPERIMENTAL MODEL AND STUDY PARTICIPANT DETAILS

We collected sporophytes of *M. quadrata* in the field (at Mt Kitadake in Minami Alps city, Japan, isolate Kitadake-1) and established an axenic culture from a single spore isolate. This plant was used in the following experiments unless otherwise stated. Under laboratory conditions, plants were grown on half-strength Gamborg's B5 medium[34] containing 1% agar or on BCD medium.[35] Plants were also grown on soil on the balcony at Kyoto University with watering provided every few days.

METHOD DETAILS

Genome assembly

Genomic DNA was isolated from the axenically grown gametophyte material using a modified CTAB protocol[36] and sequenced using PacBio HIFI technology at the Hudson Alpha Institute. The main assembly consisted of 30.35x of CCS PACBIO coverage (16,691 bp average read size) and was assembled using HiFiAsm-0.19.5-r587+HiC[37,38] and the resulting sequence was polished using RACON v1.4.3.[39] There were no misjoins identified in the polished assembly. Contigs were then oriented, ordered, and joined into chromosomes using the JUICER pipeline v1.6.[40] A total of 100% of the assembled sequence is contained in the chromosomes. Finally, Homozygous SNPs and INDELs were corrected in the release sequence using ~41.2x of Illumina reads (2x150, 400bp insert).

The nine chromosome-scale scaffolds were ordered and oriented based on the *Marchantia polymorpha* reference genome (https://marchantia.info/data/MpTak_v7.1_standard_genome/) and renamed accordingly. The smallest scaffolds of *M. quadrata*, which did not show collinearity with any *M. polymorpha* chromosome was renamed as chromosome 9. The quality of the genome assembly was assessed using BUSCO v5.6.1 (-m genome; -l embryophyta_odb10)[41] and by assessing the LTR Assembly Index (LAI)[42] with LTR_retriever v2.9.0.[43]

GetOrganelle v1.7.7.0[44] was used to assemble draft plastomes and mitogenomes. The fragmented contigs were manually anchored using their overlapped region to assemble in circular genomes in SnapGene v7.2.1. Read mapping by Minimap2 v2.28-r1209[45] was performed against both genomes and errors were manually corrected to obtain plastome (122,204 bp) and mitogenome (189,862 bp). Plastome and mitogenome were annotated by GeSeq v2.03[46] and visualized by OGDRAW v1.3.1.[47] To annotate plastome, BLAT v35.1[48] and HMMER v3.4 (hmmer.org) profile search (land plants chloroplast) for CDS, tRNA and rRNA and ARAGORN v1.2.38[49] for tRNA were used. Mitogenome was annotated with BLAT search (using *Marchantia polymorpha* subsp. ruderalis NC_037508.1 as Refseq reference) for CDS, tRNA and rRNA and ARAGORN v1.2.38 for tRNA.[49]

Genome annotation, transposable elements (TE)

For genome annotation, we extracted RNA from gametophyte tissues of about month-old plants using the Spectrum Plant Total Plant extraction kit (Sigma Aldrich). We prepared both Illumina paired-end directional and isoform sequencing (Iso-Seq) libraries which

were sequenced on Illumina Novaseqx (Illumina) and PacBio sequel IIe (PacBio) machines. In addition, we sampled thalli and archegoniophores (female receptacle) from axenic plants, whereas we collected antheridiophores (male receptacles) in the field using RNAlater (Thermo Fisher Scientific) in three biological replicates. Thalli were grown under continuous white light with a cold cathode fluorescent lamp (OPT-40C-N-L; Optrom, Miyagi, Japan) at 15°C or under short days (8 h light/16 h dark) at 4°C. Total RNA was extracted using TRIzol reagent (Thermo Fisher Scientific), treated with RNase-free DNase I (Qiagen), purified using the RNeasy Spin Column of the RNeasy Plant Mini Kit (Qiagen). RNA libraries were prepared using a NEBNext Ultra II Directional RNA Library Prep Kit for Illumina (New England Biolabs) and sequenced as single-end reads using Nextseq500 platform (Illumina). To identify gene models Braker v3.0.1[50] was run on the soft-masked *M. quadrata* genome assembly, using an alignment file that combined Illumina RNA-seq and PacBio Iso-seq transcriptomic data, and a large protein dataset that we obtained by merging OrthoDB protein dataset for Viridiplantae (odb10; www.orthodb.org) with the high-quality protein set of seven bryophyte species namely *Syntrichia caninervis, Sphagnum fallax, Ceratodon purpureus GG1, Ceratodon purpureus R40, Anthoceros angustus, Anthoceros agrestis BONN,* and *Anthoceros punctatus* (Table S5). Repetitive elements were identified in the *M. quadrata* genome assembly using RepeatModeler v2.0.3[51] and the resulting TE library was concatenated with the RepBase[52] TE library for plant species. The concatenated TE library was then used as input, together with the genome assembly, to run RepeatMasker v4.0.9 (-xsmall).[53] The Illumina RNA-seq reads were aligned onto the soft-masked assembly using HISAT v2.1.0 (–dta –max-intronlen 100000).[54] The Iso-seq data was mapped to the soft-masked assembly using Minimap v2.24 (-ax splice:hq –uf).[45] Finally, Braker3 was run using, as input: the soft-masked genome assembly; the BAM file resulting from merging the alignments of Illumina RNA-seq and PacBio Iso-seq data; the FASTA file containing the protein dataset. Genes were then renamed using the rename_gtf.py script of the TSEBRA v1.1.2.5 software[50] and the longest transcriptional isoform for each gene was identified with a custom script. The quality of the gene annotation was assessed using BUSCO v5.6.1 (-m proteome; -l embryophyta_odb10).[41] The annotated gene set was further filtered for complete gene models containing no internal stop codons and curated manually. Mono-exonic gene models were assessed in an orthofinder analyses and those with orphan orthogroups, no hits against the NCBI nr database as well as against transcriptomes of other liverworts were discarded as false positives. These gene models also did not have much transcriptomic/protein support. Transposable elements (TE) were identified using Extensive *De novo* TE Annotator (EDTA) v1.9.2,[55] a software that combines structure- and homology-based approaches for *de novo* TE identification. The repeat library created by EDTA was then used to annotate the genome assembly using RepeatMasker v4.0.9 (www.repeatmasker.org).[53]

Phylogenetic analyses of gametologs

We collected *M. polymorpha* gametolog gene pairs from published datasets[30,56] and revised this set using the latest genome version (https://marchantia.info/data/MpTak_v7.1_standard_genome/). We downloaded the respective sequence data and added the homologous *Ricciocarpos natans*[21] and *M. quadrata* gene models as well as further transcriptome sequences (Table S5) to each tree based on an OrthoFinder v2.3.11 analysis[57] (Table S6). We aligned nucleotide sequences using default parameters in muscle v5.2.[58] We manually revised the resulting alignments if necessary and reconstructed the phylogeny using IQ-TREE v2.0.6[59] applying 1000 ultrafast bootstrap support analyses and default parameters.

Comparative genomic analysis

To identify collinearity between the *M. quadrata* and *M. polymorpha* genomes we used MCScan[60] (https://github.com/tanghaibao/jcvi/wiki/MCscan-%28Python-version%29). First, we identified syntenic 'anchors' with jcvi.compara.catalog ortholog (–min_size = 4 –dist = 40). Then, we generated a succinct form of the 'anchors' file with jcvi.compara.synteny screen (–minspan = 30). Whole genome synteny and microsynteny plots were generated with the jcvi.graphics.karyotype and jcvi.graphics.synteny functions of MCScan, respectively. Orthologous gene sets were identified among ten proteomes of nine Marchantiales species (Tables S5 and S6), plus the hornwort *Anthoceros agrestis* as outgroup, using OrthoFinder v2.3.11[57] with default parameters.

Gene expression analysis

The FASTQ files from RNA-seq data using thallus grown at 15°C and sexual receptacles mentioned in the annotation section above were processed using nfcore/rnaseq pipeline v3.13.2[61] with default settings, along with –trimmer fastp option to map reads Bigwig files were generated using bamcoverage in Deeptools v3.5.6[62] with –binSize 10 –normalizeUsing BPM. FeatureCounts v2.18.0[63] was run with the -M -O -s 2 options on the bam files to accurately count reads mapped on the two identical *BPCU* genes and the *FGMYB-SUF*, which have a sense/antisense relationship. Differential expression of the *BPCU*, *BPCV*, *FGMYB* and *SUF* genes were carried out using a Tukey-Kramer test ($p < 0.05$) in R v4.1.0.[64]

Histological analysis

Tissues were fixed in formaldehyde/alcohol/acetic acid (FAA) solution under vacuum and dehydrated in a graded ethanol series. Samples were embedded in Technovit 7100 (Heraeus Kulzer) and sectioned with a microtome (HM 340E; Thermo Scientific Microm). Sections were stained with Toluidine Blue and observed under the microscope (BZ-X710; Keyence).

Chromatin conformation analysis

To calculate the decay of chromatin contacts along chromosomes, we first mapped the Omni-C reads (Cantata Bio) against the genome assembly following the protocol of Dovetail Genomics (https://omni-c.readthedocs.io/en/latest/fastq_to_bam.html). In brief, reads were mapped with BWA mem2 v2.2.1[65] activating the '-5SP' flag to a) take the alignment with the smallest coordinate (5′ end) as primary, b) skip mate rescue, and c) skip pairing. The resulting SAM file was then processed with three functions of pairtools v0.3.0,[66] in the following order: 'parse' (–min-mapq 40 –walks-policy 5unique –max-inter-align-gap 30 –chroms-path), 'sort', and 'dedup' (–mark-dups). Then, the distance between the two maps was calculated for each read pair representing intra-chromosomal chromatin contacts and plotted.

QUANTIFICATION AND STATISTICAL ANALYSIS

The quantification and statistical analyses for each experimental and computational method used were conducted as described in the individual method sections above.